Different Modes of Binding of Mono-, Di-, and Trihalogenated Phenols to the Hemoglobin Dehaloperoxidase from *Amphitrite ornata*[†]

Michael F. Davis,[‡] Hanna Gracz,[‡] Franck A. P. Vendeix,[§] Vesna de Serrano,[‡] Aswin Somasundaram,[‡] Sean M. Decatur,[||] and Stefan Franzen*[,‡]

Department of Chemistry, North Carolina State University, Raleigh, North Carolina 27606, Department of Molecular and Structural Biochemistry, North Carolina State University, Raleigh, North Carolina 27606, and Chemistry Department, Oberlin College, Oberlin, Ohio 44074

Received August 20, 2008; Revised Manuscript Received January 6, 2009

ABSTRACT: The hemoglobin dehaloperoxidase (DHP), found in the coelom of the terebellid polychaete *Amphitrite ornata*, is a dual-function protein that has the characteristics of both hemoglobins and peroxidases. In addition to oxygen transport function, DHP readily oxidizes halogenated phenols in the presence of hydrogen peroxide. The peroxidase activity of DHP is high relative to that of wild-type myoglobin or hemoglobin, but the most definitive difference in DHP is a well-defined substrate-binding site in the distal pocket, which was reported for 4-iodophenol in the X-ray crystal structure of DHP. The binding of 2,4,6-trihalogenated phenols is relevant since 2,4,6-tribromophenol is considered to be the native substrate and 2,4,6-trichlorophenol also gives high turnover rates in enzymatic studies. The most soluble trihalogenated phenol, 2,4,6-trifluorophenol, acts as a highly soluble structural analogue to the native substrate 2,4,6-tribromophenol. To improve our understanding of substrate binding, we compared the most soluble substrate analogues, 4-bromophenol, 2,4-dichlorophenol, and 2,4,6-trifluorophenol, using ^{1}H and ^{19}F NMR to probe substrate binding interactions in the active site of the low-spin metcyano adduct of DHP. Both mono- and dihalogenated phenols induced changes in resonances of the heme prosthetic group and an internal heme edge side chain, while ^{1}H NMR, ^{19}F NMR, and relaxation data for a 2,4,6-trihalogenated substrate indicate a mode of binding on the exterior of DHP. The differences in binding are correlated with differences in enzymatic activity for the substrates studied.

The terebellid polychaete *Amphitrite ornata* inhabits estuarine mudflats with other marine annelids, such as *Notomastus lobatus*, *Saccoglossus kowalevskii*, and *Thelepus crispus*, which secrete brominated aromatic compounds as a means of territorial protection (*1*−*3*). While such repellents would be deterrents for some organisms, *A. ornata* has developed a novel defense mechanism in the hemoglobin dehaloperoxidase (DHP).[1] DHP is found in the coelom of *A. ornata* and is one of two hemoglobins in the organism (*4*). Structurally, the DHP monomer is homologous to myoglobin containing the globin fold with eight helices and a heme prosthetic group ligated to the protein backbone via a proximal histidine (*5, 6*). The novelty of DHP lies in its ability to oxidatively dehalogenate haloaromatics found in its environment while simultaneously maintaining an oxygen storage function consistent with its hemoglobin structure (*7*−*9*).

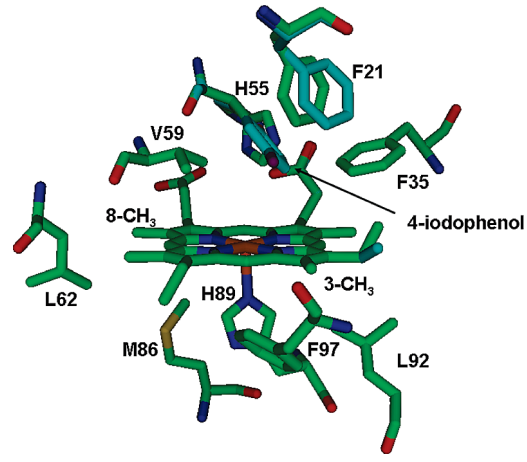

FIGURE 1: X-ray crystal structures of the local heme environment and substrate binding residues of DHP shown with (light blue) and without (green) bound substrate 4-iodophenol. Once the substrate binds, the 4-vinyl heme substituent shows slight changes in orientation. More predominant changes are observed in the orientations of His55 and Phe21.

DHP has the highest turnover rate for 2,4,6-trihalogentated phenols, which have been shown to be extremely toxic to marine life (*10, 11*).

The first X-ray crystal structure of substrate-bound DHP revealed that 4-iodophenol binds in the distal pocket but is not coordinated to the heme iron (Figure 1) (*5, 6*). This internal binding site distinguishes DHP not only from other

[†] This project was supported by Army Research Office Grant 52278-LS.

* To whom correspondence should be addressed. Phone: (919) 515-8915. Fax: (919) 515-8920. E-mail: Stefan_Franzen@ncsu.edu.

[‡] Department of Chemistry, North Carolina State University.

[§] Department of Molecular and Structural Biochemistry, North Carolina State University.

[||] Oberlin College.

[1] Abbreviations: Ap, ampicillin; 4-BP, 4-bromophenol; 2,4-DCP, 2,4-dichlorophenol; DHP, dehaloperoxidase; DHPCN, cyanide-ligated dehaloperoxidase; HRP, horseradish peroxidase; IPTG, isopropyl β-D-thiogalactopyranoside; 2,4,6-TBP, 2,4,6-tribromophenol; 2,4,6-TCP, 2,4,6-trichlorophenol; 2,4,6-TFP, 2,4,6-trifluorophenol.

10.1021/bi801568s CCC: $40.75
Published on Web 02/19/2009

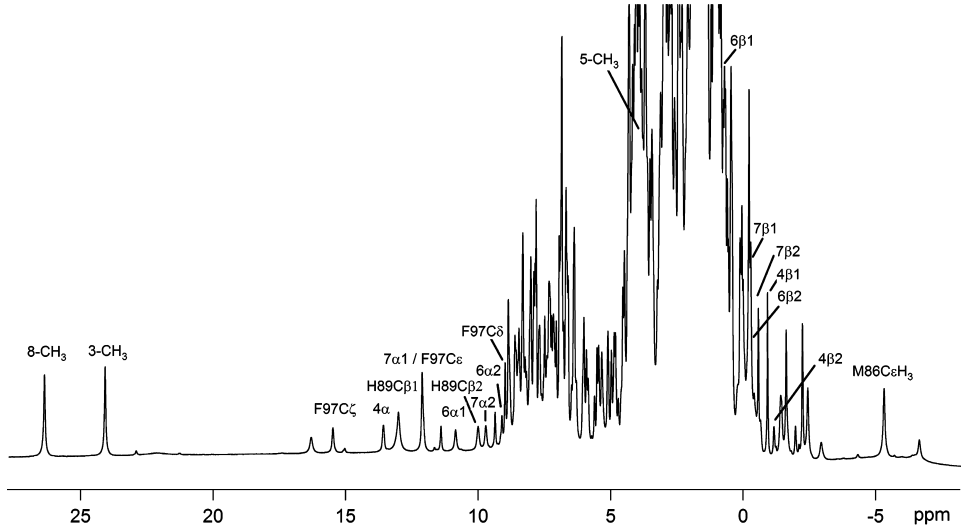

FIGURE 2: ^{1}H NMR spectrum of DHPCN. Spectrum taken at 298 K, 99.9% D_2O, 100 mM potassium phosphate, and pH 7.0. The assigned hyperfine-shifted resonances are labeled.

globins but also from other heme peroxidases that typically bind substrates on the heme periphery (*12*). According to this X-ray structure (Protein Data Bank entry 1EWA), the average occupancy of the substrate analogue 4-iodophenol in the internal binding site is only ~23% (*6*). Examination of the substrate-bound DHP crystal structure shows primary structural changes occurring solely at the heme and surrounding residues when substrate is bound. We have also confirmed by X-ray crystallography that para-halogenated (4-bromo- and 4-iodophenol) phenols can occupy this internal binding site (V. de Serrano and S. Franzen, unpublished data). However, 2,4-di- and 2,4,6-trichlorophenols do not readily enter the distal pocket in the crystal form. This is ironic considering the high turnover rate of 2,4,6-trihalophenols, which are the most active substrates for DHP. 2,4,6-Trifluorophenol (2,4,6-TFP) has been shown to enter the distal pocket of the metaquo and carbonmonoxy forms of DHP at low temperatures. We have recently shown that 2,4,6-TFP can displace the coordinated water molecule of the metaquo form at low temperature (*13*). However, it is apparently expelled from the distal pocket in the carbonmonoxy form at room temperature (*14*). The interaction of diatomic ligands and hydrogen peroxide, in the internal binding site is highly relevant to the function of DHP. The competition for binding in the distal pocket may involve the site occupied by 4-iodophenol in the 1EWA crystal structure.

We have used the carbonmonoxy form of DHP (DHPCO) as a model for the interaction of halogenated phenols and a heme-coordinated diatomic ligand in the distal pocket. 2,4,6-TFP has been observed to enter the distal pocket of the DHPCO at low temperatures at pH 5.5, but not at room temperature (*14*). We have recently shown that 2,4,6-TFP also binds to the DHPCO form at room temperature at pH 4.7 (*50*). The functional relevance of this binding is still not clear. Since trihalogenated substrates, such as 2,4,6-tribromophenol (2,4,6-TBP), exhibit the highest turnover rates, it is key from a functional perspective to determine whether oxidation of the substrate can occur in the internal site. The fact that the native substrate, 2,4,6-TBP, and other trihalophenols do not bind in that site under physiological conditions at room temperature and pH 7.4 presents a conundrum for DHP function. These data suggest that the internal binding site is not the active site. Therefore, the binding site for the native substrate, 2,4,6-TBP, has not yet been determined. The well-defined internal binding site for monohalogenated phenols, such as 4-bromophenol, may interfere with the binding of oxygen or hydrogen peroxide and could regulate either the hemoglobin or peroxidase function of DHP.

The X-ray crystal structure of DHP shows that the entire 4-iodophenol molecule binds within 6 Å of the iron center (*6*). The proximity of the internal molecular binding site to the heme permits the application of paramagnetic NMR experiments in elucidating specific structural changes near the heme iron when molecules bind in the internal binding pocket (*15*). NMR has been used extensively for active site characterization of high-spin ($S = {}^5/_2$) and low-spin ($S = {}^1/_2$) forms of many peroxidases and globins (*16*−*23*) and provides a sensitive method for probing structural details of the heme prosthetic group. Addition of a strong-field ligand, e.g., cyanide, to the ferric Fe(III) oxidation state of DHP creates a low-spin ($S = {}^1/_2$), paramagnetic species. This metcyano form is the focus of the current NMR study, as active site resonances are much sharper and less dispersed in the low-spin form than the high-spin, metaquo counterpart.

Herein, we report the first assignment and active site characterization of DHP using NMR spectroscopy and present evidence that there is both an internal and an external binding site for halogenated phenols. Assignment of the resonances was accomplished primarily through natural abundance ^{13}C−^{1}H HSQC (*24*) and WEFT-NOESY (*25*) experiments. Differential perturbation of certain active site resonances was observed upon titration of three different halogenated phenols chosen for their high water solubility: 4-bromophenol (4-BP), 2,4-dichlorophenol (2,4-DCP), and 2,4,6-trifluorophenol (2,4,6-TFP). The effects of substrate binding were also compared over a wide pH range.

MATERIALS AND METHODS

Protein Preparation. The pET 16b plasmid containing the 6XHisDHP4R DNA insert (*7*) was transformed into competent BL21(DE3) *Escherichia coli* cells, plated out on LB agar plates with 100 μg/mL ampicillin (Ap), and allowed to

grow at 37 °C for ~14 h. Single colonies were isolated, and starter growths were used to inoculate 6 L *E. coli* growths. The cells were incubated at 37 °C with shaking for 13 h. Expression of 6XHisDHP4R protein was not induced via addition of ITPG. Basal expression of the protein in the nonstringent BL21(DE3) cell line yielded significantly high levels of holoprotein. The cells were collected via centrifugation and then allowed to freeze overnight at −20 °C. The cells were resuspended in lysis buffer (2 mL/g of cell pellet) [50 mM NaH_2PO_4, 300 mM NaCl, and 10 mM imidazole (pH 6)], and lysozyme was added to a final concentration of 1 mg/mL. The cell slurry was allowed to stir at 4 °C for 1 h. The slurry was then sonicated for 30 min, and 200 μL of DNase I (16 mg/mL) and RNase A (10 mg/mL) were added. The cell slurry was again stirred at 4 °C for ~1 h before being frozen overnight at −20 °C. After rethawing, the cells were centrifuged at 18000 rpm for 45 min, and supernatant His-tagged DHP protein was collected. The crude His-DHP was applied to a Ni-NTA agarose column (Qiagen), washed with 50 mM NaH_2PO_4, 300 mM NaCl, 20 mM imidazole buffer (pH 6), and eluted with 50 mM NaH_2PO_4, 300 mM NaCl, 250 mM imidazole buffer (pH 6). The isolated His-DHP was buffer exchanged in 20 mM KH_2PO_4 (pH 6) using a Sephadex G-25 column. The protein was further purified on a CM 52 ion exchange column and was eluted stepwise between pH 6 with 20 mM KH_2PO_4 and pH 6 with 150 mM KH_2PO_4. The concentration of the protein was determined using the Soret band at 406 nm with a molar absorptivity of 116400 M^{-1} cm^{-1} (*26*). Final yields of purified wild-type (wt) DHP protein were approximately 20 mg/L of broth with A_{406}/A_{280} ratios greater than 4. Purified His-DHP was exchanged in 99.9% D_2O, 100 mM potassium phosphate buffer (pH 7). The reported pH values are left uncorrected for the deuterium isotope effect. The protein was concentrated to a final concentration of ~1−2 mM, and KCN was added to an approximately 10-fold excess.

^{1}H NMR Experiments. All ^{1}H NMR and ^{19}F NMR spectra were recorded on a either a 500 MHz AVANCE Bruker or 300 MHz Bruker NMR spectrometer. The one-dimensional (1D) NOE experiments were performed using a decoupling pulse to saturate the resonance of interest (*27*). Identical spectra were then collected with the decoupler slightly off-resonance. Difference spectra were generated by subtracting the on-resonance spectrum from the off-resonance spectrum. The magnitude of the NOE did not increase after 200 ms of resonance saturation via the decoupler. Thus, the 1D NOE data were collected in the steady state regime with a saturation time of 200 ms. The T_1 experiments were conducted using a standard inversion−recovery pulse sequence without a presaturation pulse. The τ values for the TFP relaxation experiments were 0.2, 0.4, 0.8, 1.6, 3.2, 6.4, 10, and 20 s, with a delay time, t, of 22 s. T_2 measurements were taken using a standard Carr−Purcell−Meiboom−Gill (CPMG) pulse sequence. The WEFT-NOESY data were collected utilizing a recovery delay of 300 ms and a mixing time of 100 ms. The ^{1}H−^{13}C HSQC experiments were recorded using a recycle time of 200 ms with a J of 200 Hz. Two-dimensional (2D) NOESY spectra incorporating a presaturation pulse were collected using a spectral width of 27000 Hz. Best results were obtained with a mixing time of 100 ms and a delay time of 1.2 s. Gradient-selective COSY spectra were also collected over a spectral width of 27000 Hz. A total of 2048 t_2 points and 512 t_1 blocks were collected with a delay time of 1.2 s.

Table 1: ^{1}H and ^{13}C NMR Assignments and T_1 Measurements for Selected Resonances of DHPCN at 25 °C and pH 7.0

	^{1}H δ (ppm)	^{13}C δ (ppm)	^{1}H T_1 (ms)	R_{Fe} (Å)[a]	R_{Fe} (Å)[b]
heme					
8-CH_3	26.8	−53.1	188	*c*	5.70
3-CH_3	24.5	−59.5	204	*c*	5.72
5-CH_3	4.3	−14.8	*d*	−	5.43
4α	14.0	52.8	149	5.43	5.68
4β_1	−1.1	not observed	*d*	−	6.75
4β_2	−1.5	not observed	303	6.1	6.75
6α1	13.4	84.4	−	−	5.8
6α2	9.4	84.4	−	−	6.29
6β1	1.2	not observed	*d*	−	6.23
6β2	0.3	not observed	*d*	−	7.56
7α1	12.5	−32.7	*d*	−	6.44
7α2	10.2	−32.7	213	5.76	5.83
7β1	0.4	118.8	*d*	−	6.27
7β2	−0.2	118.8	*d*	−	6.14
Phe97			−		
CζH	15.9	134.5	90	4.79	5.25
CεHs	12.6	132.6	*d*	−	5.45, 6.99
CδHs	9.4	132.2	*d*	−	7.27, 8.48
His89					
Nε_2H	19.9	not applicable	−	−	5.22
Cβ1H	13.4	24.5	*d*	−	6.45
Cβ2H	10.4	24.5	105	5.12	6.29

[a] Calculated using $R_{Fe}^i/R_{Fe}^j = (T_1^i/T_1^j)^{1/6}$. [b] Measurements taken from the X-ray structure (*5, 6*). [c] Not applicable due to contact shift contribution. [d] Not accurate measurements due to overlapping resonances.

UV−Vis Enzymatic Assays. For all experiments, the protein was exchanged into 100 mM potassium phosphate buffer (pH 7). The absorption data were collected using a Hewlett-Packard 8453 multiwavelength spectrometer. The spectra were collected every 5 s over a 60 s time frame. The conditions used for the assays were 5 μM DHP, 360 μM H_2O_2, and 120 μM substrate. Substrate turnover was monitored by the disappearance of substrate absorption bands (4-BP, 280 nm; 2,4-DCP, 284 nm; 2,4,6-TFP, 272 nm).

RESULTS

The low-spin metcyano form of DHP at pH 7.0 and 25 °C exhibits a wide dispersion of hyperfine-shifted heme and active site resonances, from −12 to 27 ppm as seen in Figure 2 and reported in Table 1. ^{13}C−^{1}H HSQC, WEFT-NOESY, gradient-selective COSY, 1D NOE difference, and presaturation NOESY spectra were used to assign the majority of active site resonances. The spectra of resonances pertinent to the substrate binding study are presented.

Examination of the X-ray structures shows that only the 3-CH_3 and 5-CH_3 heme methyls are within NOE distance of Phe side chains (*5, 6*), and only the former would have NOE connectivity to a vinyl substituent. The heme methyl at 24.5 ppm, assigned as the 3-CH_3 heme methyl, exhibits dipolar connectivity to a scalar coupled three-proton system at 14, −1.1, and −1.5 ppm, which is assigned as the vinyl 4αH and 4βH resonances, respectively (Figure 3), and dipolar connectivity to the CεH and CδH resonances of the well-resolved Phe97 side chain at 12.6 and 9.4 ppm (Table 1). The scalar coupled three-proton spin system was readily assigned as a heme vinyl group due to characteristic hyperfine shifting where the β-vinyl resonances are shifted to much lower frequencies than the α-resonance due to a large

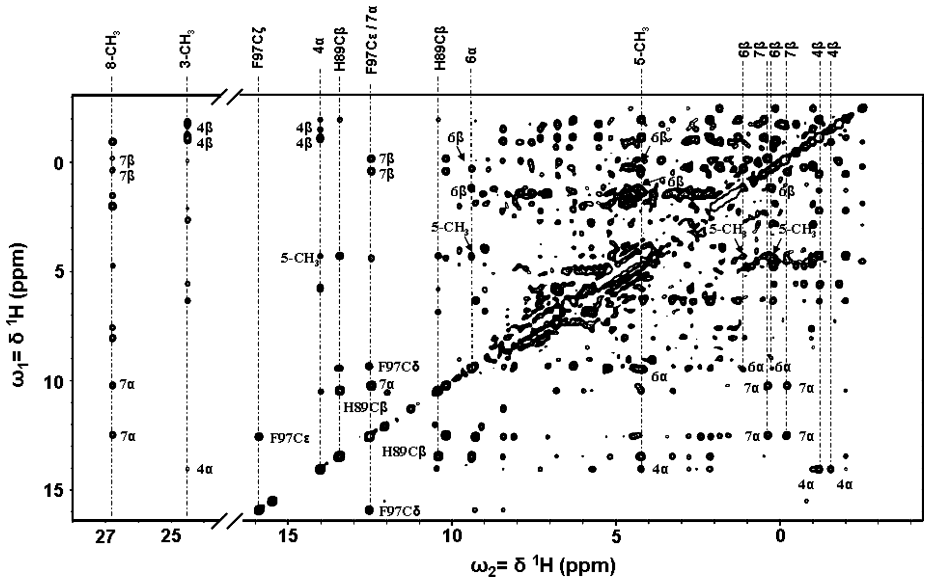

FIGURE 3: WEFT-NOESY map of metcyano DHP at 298 K, in 99.9% D_2O and 100 mM potassium phosphate, at pH 7.0. The mixing time was 100 ms. The labeled cross-peaks represent the observed ^1H dipolar connectivity.

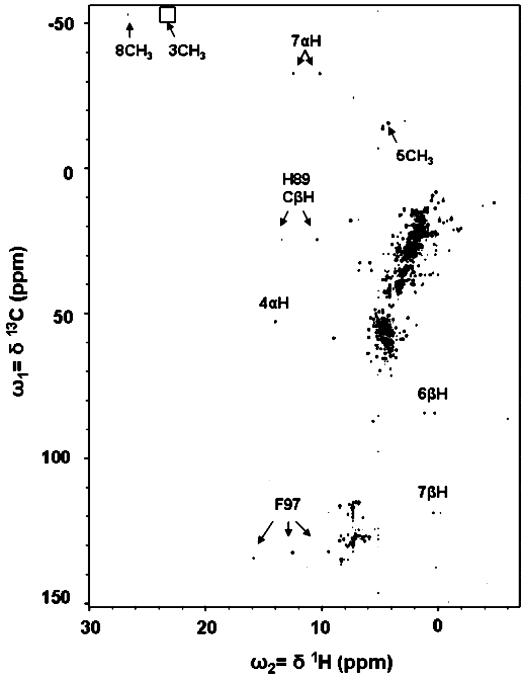

FIGURE 4: $^{13}C-^1H$ HSQC spectrum of DHPCN recorded at 298 K, in 99.9% D_2O with 100 mM potassium phosphate, at pH 7.0. Hyperfine-shifted resonances of the heme and local amino acids are labeled. The box indicates a cross-peak observed at higher contour levels.

Scheme 1: Axial Histidine Projection Angles As Shown in the X-ray Structures (A) and by the Relative Order of Heme Methyl Chemical Shifts (B)

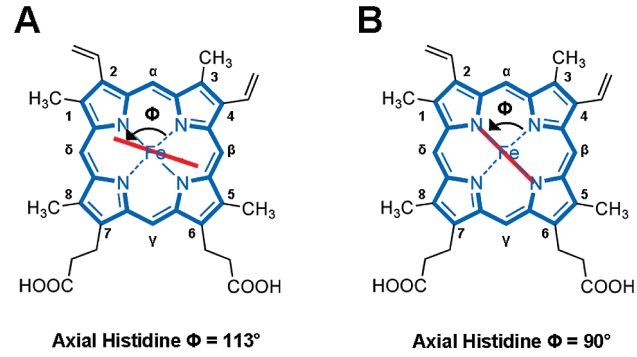

decrease in the contact shift contribution (*28*). While the 4β protons are not observed in the $^{13}C-^1H$ HSQC spectra (Figure 4), the 4α resonance was readily assigned at 14 (^1H) and 52.8 ppm (^{13}C). The Phe97 side chain was assigned by the natural abundance ^{13}C chemical shifts, CζH at 134.5, CεH at 132.6, and CεH at 132.2 ppm, and scalar coupling between the ring protons (Supporting Information).

The 4αH resonance also exhibits an NOE cross-peak to the 5-CH_3 heme methyl at 4.3 ppm. The 4.3 ppm resonance is assigned as the 5-CH_3 resonance due the degree of hyperfine shifting in the ^{13}C dimension (−14.8 ppm) and NOEs to a four-proton spin system indicative of the 6-propionate chain. This four-proton spin system at 11.3, 9.4, 1.2, and 0.3 ppm exhibits mutual dipolar coupling with the 5-CH_3 heme methyl. Only the two 6βH resonances of the propionate chain [1.2 and 0.3 ppm (84.4, ^{13}C)] were found in the $^{13}C-^1H$ HSQC map. NOESY cross-peaks of the two 6αH resonances (11.3 and 9.4 ppm) are observed at higher contour levels. Additional NOESY connectivity between the 6-propionate resonances can be found in the Supporting Information. The remaining downfield heme methyl at 26.8 ppm is assigned as the 8-CH_3 resonance on the basis of NOE connectivity to two hyperfine-shifted methylene groups at 12.5 and 10.2 ppm (−32.7, ^{13}C) and 0.4 and −0.2 ppm (118.8, ^{13}C) indicative of the 7-propionate chain. Inspection of the COSY data (Supporting Information) shows both methylene groups are scalar coupled, thus confirming their assignment as the 7αH and 7βH resonances, respectively.

The order of heme methyl shifts in metcyano DHP is 8 > 3 > 5 with the 1-CH_3 methyl not yet assigned. The 1-CH_3 methyl in low-spin metcyano heme proteins, at ambient temperatures, typically occurs at frequencies lower than those of the 5-CH_3 heme methyl. The relative order of heme methyl shifts is correlated to the angle, Φ, of the proximal histidine projection onto the $N_{II}-Fe-N_{IV}$ axis of the heme plane (*23, 29−33*). According to the X-ray structure of DHP, the axial histidine Φ is ∼113° as seen in Scheme 1A (*5, 6*). Models and experimental data have shown the 113° angle corresponds

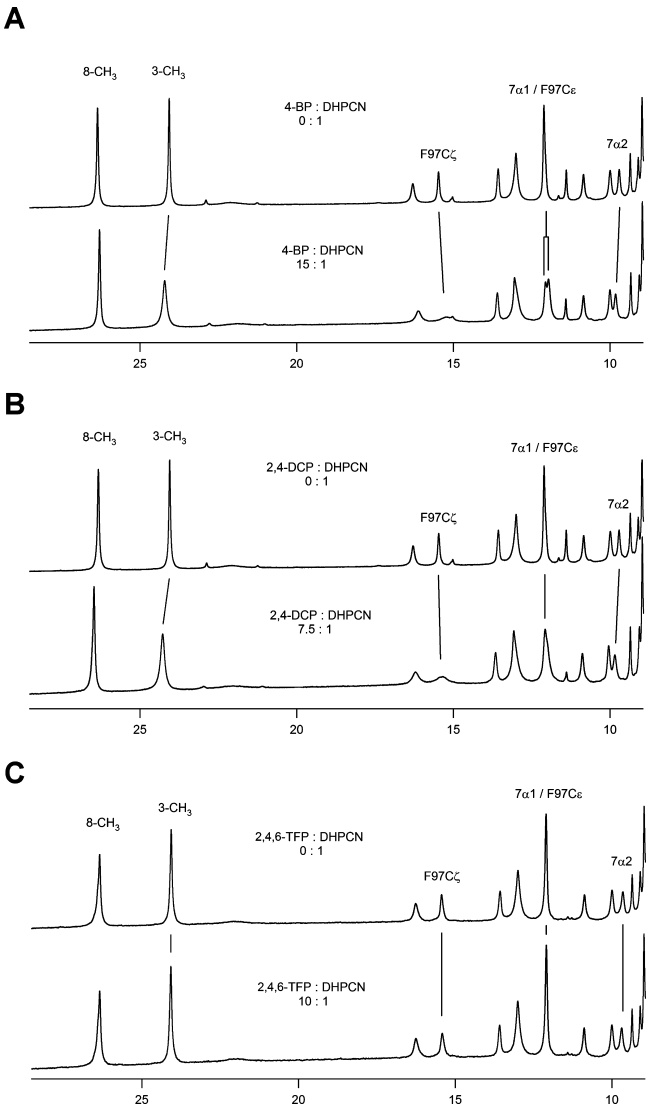

FIGURE 5: High-frequency hyperfine-shifted resonances of DHPCN in 100 mM potassium phosphate at pH 7.0 and 25 °C (A) without (top) and with (bottom) a 15-fold excess of 4-bromophenol, (B) without (top) and with (bottom) excess 2,4-dichlorophenol, and (C) without (top) and with (bottom) excess 2,4,6-trifluorophenol. Addition of either 4-BP or 2,4-DCP induces line broadening of the internal heme 3-CH_3 and Phe97 ring resonances, while the external 7α1H and 7α2H resonances show changes in their respective chemical shifts. Addition of 2,4,6-trifluorophenol does not effect any of the hyperfine-shifted resonances.

to a 3 > 8 > 5 > 1 order of heme methyls (*33*−*35*), which is not corroborated by the 8 > 3 > 5 > 1 order found in the ^{1}H NMR spectrum. Hence, the NMR data suggest the axial histidine in metcyano DHP is rotated by approximately −25° to ∼90° in solution, as seen in Scheme 1B.

Effects of Addition of Halogenated Phenols to DHPCN. The effects of three different substrates on the active site of DHPCN can be seen in Figure 5. The molecules 4-BP, 2,4-DCP, and 2,4,6-TFP were chosen for their high water solubility and/or structural similarities to substrates that have high rates of product turnover in DHP. The native substrate 2,4,6-TBP (*1*) and commonly used model substrate, 2,4,6-trichlorophenol (2,4,6-TCP) (*7*), cannot be used in the NMR binding studies due to their poor solubility. However, 4-BP is structurally comparable to 4-iodophenol, which was shown to bind in the internal distal cavity of DHP in current X-ray structures (*6*), while 2,4,6-TFP provides a comparison to the

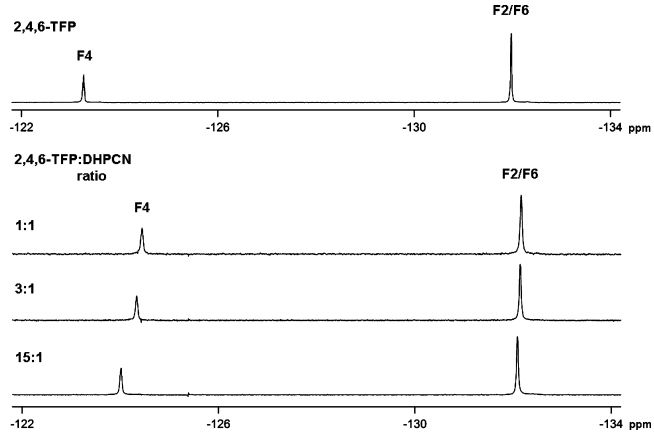

FIGURE 6: ^{19}F NMR spectra of the 2,4,6-TFP substrate analogue at pH 7 with 100 mM potassium phosphate and 99.9% D_2O buffer (top) and titration of this substrate to metcyano DHP at concentration ratios of 1:1, 3:1, and 15:1.

native substrate, 2,4,6-TBP, and the most active laboratory substrate, 2,4,6-TCP. Figure 5 shows there are two different effects induced by substrate binding. The mono- and dihalogenated 4-BP and 2,4-DCP cause similar effects within the active site of DHPCN. In both cases, the 3-CH_3 heme methyl and internal Phe97 exhibit significant line broadening when substrate is added in excess. The Phe97 side chain and heme 3-CH_3 methyl are separated by ∼4.5 Å according to the X-ray structures (*5, 6*), with the Phe side chain located slightly proximal to the 3-CH_3 heme methyl. Introduction of either 4-BP or 2,4-DCP also causes a slight change in the chemical shift of the 7α propionate resonances. The 8-CH_3 resonance exhibits a slight −0.2 ppm shift in the presence of 4-BP and a 0.1 ppm shift in the presence of 2,4-DCP. On the other hand, the interaction of 2,4,6-TFP with DHP does not create frequency perturbations and/or line broadening of active site resonances in DHPCN at the pH values studied. Comparing the effects of substrate titrations provides initial evidence for different modes of binding for substrates 2,4-DCP and 4-BP compared to 2,4,6-TFP. The differences in the nature of binding interactions are observed even when a significant molar excess of 2,4,6-TFP is used in DHPCN solutions (Supporting Information).

^{19}F NMR and Relaxation Data for Substrate 2,4,6-TFP in DHPCN. Utilization of ^{19}F NMR permits direct observation of the substrate as a probe of binding. In general, any binding interactions between the smaller 2,4,6-TFP substrate and DHP will result in a decrease in T_2 and, therefore, an increase in line width due to a slower molecular tumbling rate. Alternatively, depending on the rate of exchange, separate resonances may be visible for the fluorinated substrate, one for both the bound and free state of the substrate (*36, 37*).

Figure 6 shows the ^{19}F NMR spectra of substrate 2,4,6-TFP and titration of 2,4,6-TFP to the fully formed DHPCN complex. A significant change in chemical shift is observed in the para (F4) resonance as it is titrated to DHP. The F4 resonance of TFP, at −123.2 ppm, shifts to −124.4 ppm when the substrate is introduced at a 1:1 ratio. Additionally, the ortho (F2/F6) resonance shifts from −131.2 to −132.1 ppm. During the course of the titration, the F4 and F2/F6 resonances shift to slightly higher frequencies and approach the chemical shifts of 2,4,6-TFP without the presence of protein. Slight broadening of both resonances is observed at 1:1 and 3:1 ratios of 2,4,6-TFP to DHPCN. The F4 resonance

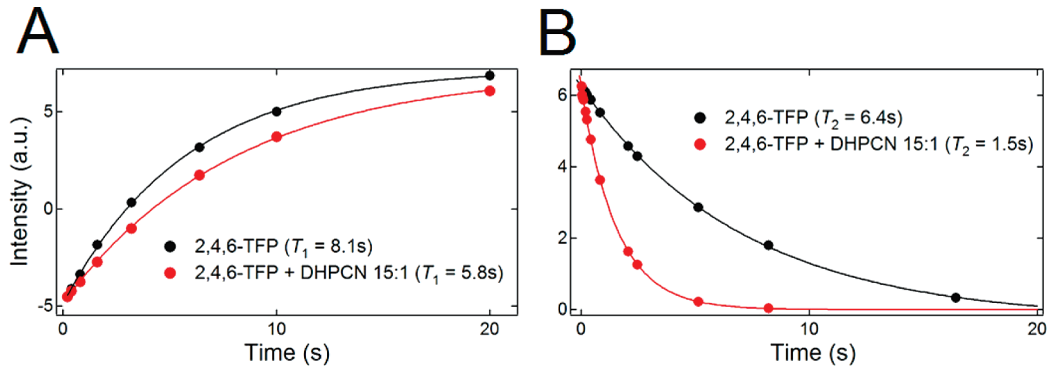

FIGURE 7: (A) T_1 relaxation curves and (B) T_2 relaxation curves for the meta protons of 2,4,6-trifluorophenol, alone (black), and in the presence of DHPCN (red) at a 15:1 molar ratio.

exhibits a 17% increase in line width (from 24 to 28 Hz), while the line width of the F2/F6 resonance increases by 33% (from 18 to 24 Hz) at a 1:1 ratio. Panels A and B of Figure 7 illustrate the change spin−lattice relaxation (T_1) and transverse relaxation (T_2) times of the 2,4,6-TFP meta protons when the molecule is added to DHPCN, respectively. The T_1 time decreased from 8.1 to 5.8 s and the T_2 time from 6.4 to 1.5 s when 2,4,6-TFP is added to DHPCN at a 15:1 molar ratio, respectively.

Enzymatic Activity Assay for Substrates 4-BP, 2,4-DCP, and 2,4,6-TFP. The hypothesis that there are two modes of binding is supported by the significant difference in the reactivity of the three phenols studied in enzymatic assays (see the Supporting Information). Using a standard DHP assay, we found that 4-BP has little or no activity. On the other hand, 2,4,6-TFP is a good substrate and shows turnover at rates that are comparable to that of the native substrate, 2,4,6-TBP (*49*). The rate of 2,4,6-TFP oxidation is approximately 3 times slower than that of the widely used test substrate, 2,4,6-TCP (*48, 49*). By contrast, 2,4-DCP shows significantly less activity than the 2,4,6-trihalophenols. There is also an increase in the baseline due to scattering when this substrate is used, which may be indicative of polymerization or other side reactions. Thus, the internal and external binding observed in the NMR signals is correlated with differences in substrate reactivity such that 4-BP and 2,4-DCP, which bind in the internal site, are not highly active and 2,4,6-TFP, which interacts with the protein at an external site, is active.

DISCUSSION

The dehalogenation of a variety of halogenated phenols, including bromo-, chloro-, and even fluorophenols, by DHP was first reported in 1996 (*2*). It was subsequently revealed that the original turnover numbers are not accurate (*8*). The X-ray crystal structure revealed the binding of 4-iodophenol in the distal pocket, which was assigned as the active site (*3*). The native substrate, however, is considered to be 2,4,6-TBP, and there has been no report of dehalogenation of 4-halophenols by DHP. This study uses soluble halogenated phenols to systematically test the differences in binding and correlated activity of three types of halogenated phenols. The molecules, 4-BP and 2,4-DCP, appear to bind or at least interact at an interior site in DHPCN and are poor substrates in a typical ferric DHP peroxidase assay using H_2O_2. On the other hand, 2,4,6-TFP interacts with the protein at an exterior site and has activity comparable to that of the native substrate, 2,4,6-TBP. In retrospect, this result is not surprising, since most known peroxidases have exterior substrate binding sites (*12*).

Binding of the monohalogenated (4-BP) and dihalogenated (2,4-DCP) substrates demonstrated comparable effects on the ^{1}H NMR spectrum of the metcyano adduct of DHP. The effects include perturbations along the internal heme edge near the 3-CH_3 heme methyl and Phe97 side chain. The broadening of these resonances appears to be greatest when the solution pH < pK_a of the substrate (Supporting Information). However, even at alkaline pH (pH 9.9), there is still observable broadening associated with the addition of 4-BP and 2,4-DCP. The effect of 4-BP and 2,4-DCP binding is localized to an internal region near the heme 3-CH_3 methyl and Phe97 residue. There is no broadening of other active site resonances, such as the 8-CH_3 methyl. Broadening of specific resonances of the heme and its substituents has been observed previously in substrate binding studies of horseradish peroxidase (HRP). Titration of the substrate benzohydroxamic acid to HRPCN resulted in significant broadening of the 8-CH_3 heme methyl and a 7α-propionate resonance, in a manner similar to the observed broadening of the 3-CH_3 and Phe97 resonances in DHPCN (*39*−*41*). Substrate binding is known to be external to the distal pocket in HRP. However, the 3-CH_3 and Phe97 resonances are more deeply buried than the 8-CH_3 heme methyl and 7α protons in DHP. Consequently, the binding interactions between 4-BP/2,4-DCP and DHPCN appear to occur at the internal site in the distal pocket. On the other hand, WEFT-NOESY and presaturation NOESY experiments did not reveal NOEs between DHPCN and the substrate analogues, 4-BP and 2,4,-DCP. The lack of NOEs may be due to fast exchange of the substrate between bound and free states. These experiments suggest that the binding of 4-BP and 2,4-DCP in the distal pocket of DHPCN may involve rapid exchange with solvent.

While the addition of 4-BP and 2,4-DCP induced observable changes in active site resonances, 2,4,6-TFP essentially had no effect on the ^{1}H NMR spectrum. The ^{19}F NMR data, however, show that the F2/F6 and F4 fluorine resonances of 2,4,6-TFP exhibit slight broadening and perturbations in chemical shifts when present at a 1:1 molar ratio with DHPCN. Resonance broadening and/or changes in chemical shift are commonly used to identify binding of small molecule protein ligands (*42*−*44*). The line width of the F2/F6 and F4 resonances at a 1:1 molar ratio of DHPCN to 2,4,6-TFP increases by 33 and 17%, respectively. This broadening translates to a decrease in the apparent transverse

relaxation time (T_2) from 17.7 to 13.3 ms for F2/F6 and from 13.3 to 11.4 ms for F4 (*45*) as discussed in the Supporting Information. The decrease in T_2 suggests a longer rotational correlation time (τ_c) of the molecule (*46*). On the basis of the Stokes−Einstein equation, $\tau_c = 34$ ns for DHPCN assuming that the radius $r = 20$ Å at a viscosity of 1 cP, whereas free 2,4,6-TFP would be expected to have a τ_c on the picosecond time scale (see the Supporting Information).

To elucidate the binding of 2,4,6-TFP to DHPCN, T_1 and T_2 relaxation experiments were used to observe changes in the rotational correlation time, τ_c. The T_1 relaxation time of the 2,4,6-TFP meta protons decreased from 8.1 to 5.8 s and the T_2 relaxation time of these same resonances from 6.4 to 1.5 s when 2,4,6-TFP was present at a 15:1 molar ratio (Figure 7). The high ratio of TFP to DHPCN was needed to fully resolve the 2,4,6-TFP signal over the background of the protein resonances. Because the same value for T_1 is consistent with two separate rotational correlation times in the limits $\omega_o\tau_c \ll 1$ and $\omega_o\tau_c \gg 1$, T_2 values were analyzed to determine whether the decrease in T_1 can be attributed to a significant decrease in the τ_c of 2,4,6-TFP in the presence of DHPCN (*47*). The analysis of the decrease in T_1 and T_2 times corresponds to a τ_c of ~35 ps for free 2,4,6-TFP and a τ_c of ~53 ns for 2,4,6-TFP in the presence of DHPCN. This increase in τ_c is in accord with the expected value for complexation of 2,4,6-TFP to DHPCN. Further details of the analysis are supplied in the Supporting Information. Although the analysis is based on a single dipolar interaction of a ^{19}F nucleus that is 2.47 Å from the meta hydrogen nucleus, we recognize that the relaxation may be more complicated in the bound state. The point of the analysis is to establish the 2,4,6-TFP binds at an external site and exhibits behavior different from that of the other two phenols studied, 4-BP and 2,4-DCP.

Although the relaxation data are consistent with an external binding site for 2,4,6-TFP, the location of that site has not been determined on the basis of the data obtained here. FTIR studies at cryogenic temperatures showed that 2,4,6-TFP can bind in the internal substrate binding pocket of the CO form of ferrous DHP, which is isoelectronic with DHPCN (*14*). However, at physiologically relevant pHs, there was no binding of 2,4,6-TFP above 260 K in the internal site (*14*). At room temperature, 2,4,6-TFP binding in the distal pocket is also observed in the CO form using FTIR, but only at pH <4.7 (*50*). It is difficult to study DHPCN at pH <5.0 to investigate the relevance of this observation using NMR due to the protonation of CN^- to form HCN. The ^{1}H NMR data corroborate the FTIR data in that no observable internal pocket perturbations are observed for the trihalogenated substrate at ambient temperatures in the pH range from 5.5 to 9.9.

The origin of the alteration of the axial histidine torsion angle shown in Scheme 1 requires further explanation. The value of the torsion angle (Φ) of ~113° shown in Scheme 1A was obtained by X-ray crystallography. The X-ray structures further indicate stabilization of the proximal histidine H89 by a strong hydrogen bond of the imidazole NH group to the carbonyl oxygen of L83 with a N···O distance of 2.74 Å (*5, 6*). The Φ value of ~90° in solution (Scheme 1B) is based on the well-established correlation of the ordering of heme methyl hyperfine shifts. The discrepancy in these data may arise from the dynamics of H89 and associated amino acid residues. The average thermal factors for amino acid residues 87−92, a region which includes the proximal histidine H89, were observed to be 50% larger than the average value in DHP as a whole (*5*). The region near H89 has the largest thermal motion in the molecule despite the fact that it is buried in the interior of the protein and bonded to the heme cofactor. The flexibility of H89 could be the reason for the decrease in the axial histidine torsion angle (Φ) from 113° to 90°, which was determined by the spacing and 8 > 3 > 5 > 1 order of heme methyl chemical shifts in the ^{1}H NMR spectrum. Similar deviations in the proximal histidine plane orientation between X-ray and solution structures have been observed in mouse neuroglobin (*38*), where higher thermal factors in the region of the proximal histidine indicated greater flexibility.

CONCLUSION

This study has shown that substrates interact with the six-coordinate DHPCN form in two different ways. Binding of both 4-BP and 2,4-DCP affects internal amino acid residues and heme group substituents in a pH-dependent manner, with the greatest affinity occurring under acidic conditions. The NMR data suggest that the binding has a strong and specific effect on the heme, which may result from an internal binding site where the substrate analogue is in rapid exchange with solvent. The molecules 4-BP and 2,4-DCP and greatly reduced in activity when compared to 2,4,6-trihalogenated phenols (*7, 48*), including 2,4,6-TFP (Supporting Information and ref *49*). Binding of 2,4,6-TFP, which is a structural homologue of the native substrate 2,4,6-TBP, did not induce effects on the internal amino acid residues, as indicated by ^{1}H NMR. However, broadening and chemical shift perturbations of the fluorine resonances are consistent with an external binding interaction. In the presence of DHPCN, the rotational correlation time of 2,4,6-TFP was found to increase from the picosecond to nanosecond time scale, consistent with the hypothesis that there is an external binding site. Although 2,4,6-TBP is not sufficiently soluble to permit a ^{1}H NMR study, the conclusion that 2,4,6-TFP binds at an external site clearly implies that the native substrate, 2,4,6-TBP, also binds at an external site. The similar reactivity of both of these substrates leads us to conclude that the active site for substrate oxidation in DHP is an external site, as observed in other heme peroxidases.

SUPPORTING INFORMATION AVAILABLE

1D NOE, gradient-selective COSY, presaturation NOESY data, variable-temperature ^{1}H NMR spectra, and hyperfine-shifted resonances in response to varying pH; additional titrations of substrate 2,4,6-TFP at alternative pHs; equations used for analysis of relaxation data; and spectroscopic data for enzyme assays of 4-BP, 2,4-DCP, and 2,4,6-TFP. This material is available free of charge via the Internet at http://pubs.acs.org.

REFERENCES

1. Han, K., Woodin, S. A., Lincoln, D. E., Fielman, K. T., and Ely, B. (2001) *Amphitrite ornata*, a marine worm, contains two dehaloperoxidase genes. *Mar. Biotechnol. 3*, 287–292.
2. Chen, Y. P., Woodin, S. A., Lincoln, D. E., and Lovell, C. R. (1996) An unusual dehalogenating peroxidase from the marine terebellid polychaete *Amphitrite ornata*. *J. Biol. Chem. 271*, 4609–4612.

3. Lebioda, L., LaCount, M. W., Zhang, E., Chen, Y. P., Han, K., Whitton, M. M., Lincoln, D. E., and Woodin, S. A. (1999) Protein structure: An enzymatic globin from a marine worm. *Nature 401*, 445.
4. Weber, R. E., Magnum, C. P., Steinman, H., Bonaventura, C., Sullivan, B., and Bonaventura, J. (1977) Hemoglobins of two terebellid polychaetes: *Enoplobranchus sanguineus* and *Amphitrite ornata*. *Comp. Biochem. Physiol. 56A*, 179–187.
5. de Serrano, V., Chen, Z., Davis, M. F., and Franzen, S. (2007) X-ray crystal structural analysis of the binding site in the ferric and oxyferrous forms of the recombinant heme dehaloperoxidase cloned from *Amphitrite ornata*. *Acta Crystallogr. D63*, 1094–1101.
6. Zhang, E., Chen, Y. P., Roach, M. P., Lincoln, D. E., Lovell, C. R., Woodin, S. A., Dawson, J. H., and Lebioda, L. (1996) Crystallization and initial spectroscopic characterization of the heme-containing dehaloperoxidase from the marine polychaete *Amphitrite ornata*. *Acta Crystallogr. D52*, 1191–1193.
7. Belyea, J., Gilvey, L. B., Davis, M. F., Godek, M., Sit, T. L., Lommel, S. A., and Franzen, S. (2005) Enzyme function of the globin dehaloperoxidase from *Amphitrite ornata* is activated by substrate binding. *Biochemistry 44*, 15637–15644.
8. Osborne, R. L., Taylor, L. O., Han, K. P., Ely, B., and Dawson, J. H. (2004) *Amphitrite ornata* dehaloperoxidase: Enhanced activity for the catalytically active globin using MCPBA. *Biochem. Biophys. Res. Commun. 324*, 1194–1198.
9. Lebioda, L. (2000) The honorary enzyme haemoglobin turns out to be a real enzyme. *Cell. Mol. Life Sci. 57*, 1817–1819.
10. Kishino, T., and Kobayashi, K. (1995) Relation between toxicity and accumulation of chlorophenols at various pH, and their absorption mechanism in fish. *Water Res. 29*, 431–442.
11. Allonier, A., Khalansk, M., Camel, V., and Bermond, A. (1999) Characterization of chlorination by-products in cooling effluents of coastal nuclear power stations. *Mar. Pollut. Bull. 38*, 1232–1241.
12. Ator, M. A., and Ortiz de Montellano, P. R. (1987) Protein control of prosthetic heme reactivity. Reaction of substrates with the heme edge of horseradish peroxidase. *J. Biol. Chem. 262*, 1542–1551.
13. Smirnova, T. I., Weber, R. T., Davis, M. F., and Franzen, S. (2008) Substrate binding triggers a switch in the iron coordination in dehaloperoxidase from *Amphitrite ornata*: HYSCORE experiments. *J. Am. Chem. Soc. 130*, 2128–2129.
14. Nienhaus, K., Deng, P. C., Belyea, J., Franzen, S., and Nienhaus, G. U. (2006) Spectroscopic study of substrate binding to the carbonmonoxy form of dehaloperoxidase from *Amphitrite ornata*. *J. Phys. Chem. B 110*, 13264–13276.
15. La Mar, G. N., and de Ropp, J. S. (1993) in *Biological Magnetic Resonance*, pp 1−73, Plenum Press, New York.
16. Emerson, S. D., and La Mar, G. N. (1990) Solution structural characterization of cyanometmyoglobin: Resonance assignment of heme cavity residues by two-dimensional NMR. *Biochemistry 29*, 1545–1556.
17. Banci, L., Bertini, I., Turano, P., Ferrer, J. C., and Mauk, A. G. (1991) Comparative ^{1}H NMR study of ferric low-spin cytochrome-c peroxidase and horseradish-peroxidase. *Inorg. Chem. 30*, 4510–4516.
18. Yu, L. P., La Mar, G. N., and Rajarathnam, K. (1990) ^{1}H NMR resonance assignments of the active site residues of paramagnetic proteins by 2D bond correlation spectroscopy: Metcyanomyoglobin. *J. Am. Chem. Soc. 112*, 9527–9534.
19. Yamamoto, Y., Iwafune, K., Nanai, N., Akemi, O., Chujo, R., and Suzuki, T. (1991) NMR study of *Galeorhinus japonicus* myoglobin. ^{1}H NMR study of molecular structure of the heme cavity. *Eur. J. Biochem. 198*, 299–306.
20. Bertini, I., Turano, P., and Vila, A. J. (1993) Nuclear magnetic resonance of paramagnetic metalloproteins. *Chem. Rev. 93*, 2833–2932.
21. Satterlee, J. D., and Erman, J. E. (1991) Proton NMR assignments of heme contacts and catalytically implicated amino acids in cyanide-ligated cytochrome c peroxidase determined from one- and two-dimensional nuclear overhauser effects. *Biochemistry 30*, 4398–4405.
22. Sukits, S. F., and Satterlee, J. D. (1996) Assignment of ^{1}H and ^{13}C hyperfine-shifted resonances for tuna ferricytochrome c. *Biophys. J. 71*, 2848–2856.
23. Shokhireva, T. Kh., Shokhirev, N. V., and Walker, F. A. (2003) Assignment of heme resonances and determination of the electronic structures of high- and low-spin nitrophorin 2 by ^{1}H and ^{13}C NMR spectroscopy: An explanation of the order of heme methyl resonances in high-spin ferriheme proteins. *Biochemistry 42*, 679–693.
24. Maudsley, A. A., and Ernst, R. R. (1977) Indirect detection of magnetic resonance by heteronuclear two-dimensional spectroscopy. *Chem. Phys. 50*, 368–372.
25. Patt, S. L., and Sykes, B. D. (1972) Water Eliminated Fourier Transform NMR Spectroscopy. *J. Chem. Phys. 56*, 3182–3184.
26. Osborne, R. L., Sumithran, S., Coggins, M. K., Chen, Y., Lincoln, D. E., and Dawson, J. H. (2006) Spectroscopic characterization of the ferric states of *Amphitrite ornata* dehaloperoxidase and *Notomastus lobatus* chloroperoxidase: His-ligated peroxidases with globin-like proximal and distal properties. *J. Inorg. Biochem. 100*, 1100–1108.
27. Satterlee, J. D., Erman, J. E., and DeRopp, J. S. (1987) Proton hyperfine resonance assignments in cyanide-ligated cytochrome *c* peroxidase using the nuclear Overhauser effect. *J. Biol. Chem. 262*, 11578–11583.
28. Alam, S. L., and Satterlee, J. D. (1994) Complete heme proton hyperfine resonance assignments of the *Glycera dibrachiata* component IV metcyano monomer hemoglobin. *Biochemistry 33*, 4008–4018.
29. Decatur, S. M., and Boxer, S. G. (1995) ^{1}H NMR characterization of myoglobins where exogenous ligand replace the proximal histidine. *Biochemistry 34*, 2122–2129.
30. Thanabal, V., de Ropp, J. S., and La Mar, G. N. (1987) ^{1}H NMR study of the electronic and molecular structure of the heme cavity in horseradish peroxidase. Complete heme resonance assignments based on saturation transfer and nuclear Overhauser effects. *J. Am. Chem. Soc. 109*, 265–272.
31. Yamamoto, Y., Nanai, N., Chujo, R., and Suzuki, T. (1990) Heme methyl hyperfine shift pattern as a probe for determining the orientation of the functionally relevent proximal histidyl imidazole with respect to the heme in hemoproteins. *FEBS Lett. 264*, 113–116.
32. Traylor, T. G., and Berzinis, A. P. (1980) Hemoprotein models: NMR of imidazole chelated protohemin cyanide complexes. *J. Am. Chem. Soc. 102*, 2844–2846.
33. Shokhirev, N. V., and Walker, F. A. (1998) The effect of axial ligand plane orientation on the contact and pseudocontact shifts of low-spin ferriheme proteins. *J. Biol. Inorg. Chem. 3*, 581–594.
34. ShiftPatterns. Heme methyl shift patterns, version 2, http://www.shokhirev.com/nikolai/programs/prgsciedu.html.
35. Banci, L., Bertini, I., Pierattelli, R., Tien, M., and Vila, A. J. (1995) Factoring of the hyperfine shifts in the cyanide adduct of lignin peroxidase from *P. chrysosporium*. *J. Am. Chem. Soc. 117*, 8659–8667.
36. Crull, G. B., Kennington, J. W., Garber, A. R., Ellis, P. D., and Dawson, J. H. (1989) ^{19}F nuclear magnetic resonance as a probe of the spatial relationship between the heme iron of cytochrome p-450 and its substrate. *J. Biol. Chem. 264*, 2649–2655.
37. Decatur, S. M., DePillis, G. D., and Boxer, S. G. (1996) Modulation of protein function by exogenous ligands in protein cavities: CO binding to a myoglobin cavity mutant containing unnatural proximal ligands. *Biochemistry 35*, 3925–3932.
38. Walker, F. A. (2006) The heme environment of mouse neuroglobin: Histidine plane orientations obtained from solution NMR and EPR spectroscopy as compared with X-ray crystallography. *J. Biol. Inorg. Chem. 11*, 391–397.
39. La Mar, G. N., Hernandez, G., and de Ropp, J. S. (1992) ^{1}H NMR investigation of the influence of interacting sites on the dynamics and thermodynamics of substrate and ligand binding to horseradish peroxidase. *Biochemistry 31*, 9158–9168.
40. Thanabal, V., de Ropp, J. S., and La Mar, G. N. (1987) Identification of the catalytically important amino acid residue resonances in ferric low-spin horseradish peroxidase with nuclear Overhauser effect measurements. *J. Am. Chem. Soc. 109*, 7516–7525.
41. de Ropp, J. S., Mandal, P. K., and La Mar, G. N. (1999) Solution ^{1}H NMR investigation of the heme cavity and substrate binding site in cyanide-inhibited horseradish peroxidase. *Biochemistry 38*, 1077–1086.
42. Reibarkh, M., Malia, T. J., and Wagner, G. (2006) NMR distinction of single- and multiple-mode binding of small-molecule protein ligands. *J. Am. Chem. Soc. 128*, 2160–2161.
43. Matsuo, H., Walters, K. J., Teruya, K., Tanaka, T., Gassner, G. T., Lippard, S. J., Kyogoku, Y., and Wagner, G. (1999) Identification by NMR spectroscopy of residues at contact surfaces in large,

slowly exchanging macromolecular complexes. *J. Am. Chem. Soc. 121*, 9903–9904.
44. Reibarkh, M., Malia, T. J., Hopkins, B. T., and Wagner, G. (2006) Identification of individual protein-ligand NOEs in the limit of intermediate exchange. *J. Biomol. NMR. 36*, 1–11.
45. Evans, J. N. S. (1995) in *Biomolecular NMR Spectroscopy*, pp 240, Oxford University Press, Oxford, U.K.
46. Tengel, T., Fex, T., Emtenäs, H., Almqvist, F., Sethson, I., and Kiflber, J. (2004) Use of ^{19}F NMR spectroscopy to screen chemical libraries for ligands that bind to proteins. *Org. Biomol. Chem. 2*, 725–731.
47. Carrington, A., and MacLachlan, A. D. (1967) in *Introduction to Magnetic Resonance*, pp 176203.
48. Franzen, S., Gilvey, L. B., and Belyea, J. (2007) The pH dependence of the activity of dehaloperoxidase from *Amphitrite ornata*. *Biochim. Biophys. Acta 1774*, 121–130.
49. Chaudhary, C. (2003) Point Mutagenesis and Spectroscopic Probing of Dehaloperoxidase: Characterizing the Mechanism and Activity of the Heme Active Site of the Native Protein, M.S. Thesis, North Carolina State University, Raleigh, NC.
50. Nienhaus, K., Nickel, E., Davis, M. F., Franzen, S., and Nienhaus, G. U. (2008) Determinants of substrate internalization in the distal pocket of dehaloperoxidase hemoglobin of *Amphitrite ornata*. *Biochemistry 47*, 12985–12994.

BI801568S